IR laser-induced decomposition of prop-2-enylsilane and ethynylsilane for chemical vapour deposition of Si/C phases

Josef Pola,*[,a] Josef Vítek,[a] Zdeněk Bastl,[b] M. Urbanová,[a] Jan Šubrt[c] and Roger Taylor[d]

[a]*Institute of Chemical Process Fundamentals, 165 02 Prague, Academy of Sciences of the Czech Republic, Czech Republic*

[b]*J. Heyrovský Institute of Physical Chemistry, 182 23 Prague, Academy of Sciences of the Czech Republic, Czech Republic*

[c]*Institute of Inorganic Chemistry, 250 68 Řež, Academy of Sciences of the Czech Republic, Czech Republic*

[d]*The School of Chemistry, Physics and Environmental Science, The University of Sussex, Falmer, Brighton, UK BN1 9QJ*

IR multiphoton decomposition of prop-2-enylsilane affords a solid material consisting of an Si/C/H polymer and SiC, while that of ethenylsilane produces a solid material consisting almost exclusively of SiC.

Thermal and photolytic decomposition of various organylsilanes $RSiH_3$ (R = alkyl, alkenyl, phenyl) is of current interest because of the use of organosilicon molecules for chemical vapour deposition (CVD) of silicon- and silicon carbide-based phases (*e.g.* ref. 1–7) which proved useful as wide band-gap materials. Various Si/C/H films, the composition of which was affected by the structure of the precursor and photolysis parameters, were deposited at low substrate temperatures by tuning laser radiation into various organosilanes.[1,6–12] UV laser-induced photolysis of monoorganylsilanes $RSiH_3$ (R = $H_2C{=}CH$, $HC{\equiv}C$, $ClHC{=}CH$, $H_2C{=}CHCH_2$) affords polycarbosilanes which are poor in hydrogen and may contain SiC.[13] These monoorganylsilanes are eminently good absorbers of CO_2 laser radiation. IR multiphoton decomposition (IRMPD) of $RSiH_3$ ($R = ClHC{=}CH$) has indeed proved a very efficient method for CVD of phases consisting of Si/C/H polymer and SiC.[14]

Intrigued by the possibility of utilizing the IRMPD of an organosilane for direct deposition of pure SiC (or a material wherein SiC is very predominant), we were continuing our studies of IRMPD of monoorganylsilanes and in this paper we report on the IRMPD of $RSiH_3$ ($R = H_2C{=}CHCH_2$ and $HC{\equiv}C$). We show that laser-induced decomposition of prop-2-enylsilane is suitable to produce deposits with high contents of SiC, and that that of ethenylsilane is unique in affording a solid deposit consisting almost exclusively of SiC.

Experimental

IRMPD experiments were performed on gaseous samples of prop-2-enylsilane ($H_2C{=}CHCH_2SiH_3$, PS) and ethynylsilane ($HC{\equiv}CSiH_3$, ES) using a TEA CO_2 laser (P. Hilendarski Plovdiv University) operating on the P(34) (931.0 cm^{-1}) and P(20) (944.2 cm^{-1}) lines of the $00^01 \rightarrow 10^00$ transition, respectively. The wavelengths were checked using a model 16-A spectrum analyser (Optical Eng. Co.) and the laser energy was determined by a pyroelectric ml-1 JU detector (Charles University).

The samples were irradiated in a Pyrex cylinder (10 cm long, 3.6 cm id) furnished with two NaCl windows and a side-arm with rubber septum. The cell accommodated Cu and NaCl substrates which, covered with the solid deposited material, were transferred for measurements of their properties by scanning electron microscopy and FTIR, XPS and XAES spectroscopy.

Chemical changes after the laser radiation were monitored directly in the cell by an FTIR (Nicolet, model Impact 400) spectrometer. The depletion of PS and ES was followed by using absorption bands at 1643 cm^{-1} (absorption coefficient 0.016 $kPa^{-1}\,cm^{-1}$) and 1341 cm^{-1} (absorption coefficient 0.013 $kPa^{-1}\,cm^{-1}$), respectively. Ethyne, silane and methane were monitored, in the given order, at 729, 2185 and 1304 cm^{-1}. GC–MS and GC analyses of the gaseous samples after the irradiation were conducted on a Shimadzu model QP 1000 quadrupole spectrometer and on a Shimadzu 14 A chromatograph coupled with a Chromatopac C-R5A computing integrator and equipped with Porapak P and SE-30 columns using programmed temperature (20–150 °C) and helium or nitrogen carrier gas.

The XPS and XAES analyses were conducted with a VG ESCA 3 Mk II electron spectrometer employing Al-Kα X-rays. X-Ray excited Auger electron spectra were obtained using Bremsstrahlung radiation. The Auger spectra were measured for the purpose of calculating the modified Auger parameter which, besides being an important source of chemical information, is independent of the reference level and possible static charging of the sample. The electron spectra were obtained with the sample at an angle of 45° with respect to the analyser axis. The spherical sector analyser was operated in the fixed analyser transmission mode using a pass energy of 20 eV corresponding to Au $4f_{7/2}$ FWHM of 1.2 eV. The analyser was calibrated to the Au $4f_{7/2}$ line at 84.0 eV. The samples in the form of deposits on copper plates were mounted on a sample probe by means of tantalum clips. Detailed spectral scans were taken over Si 2p, Si ($KL_{23}L_{23}$), C 1s and O 1s regions. Pressure of residual gases during spectra measurements did not exceed 10^{-6} Pa. The photoelectron spectra treatment procedure involved the following steps: (i) $K\alpha_{3,4}$ components were removed, (ii) a non-linear Shirley type[15] background was subtracted, (iii) overlapping spectral peaks were resolved into individual components using the damped non-linear least-squares technique[16] and lines of Gaussian–Lorentzian shape. Quantification of the element surface concentration ratio was accomplished by correcting integral intensities of photoelectron lines for their cross-sections[17] and accounting for the dependence of analyser transmission[18] and electron mean free paths[19] on the kinetic energy of photoelectrons. The accuracy of the measured binding energies was ± 0.2 eV.

SEM studies of the deposits were performed on an ultrahigh vacuum Tesla BS 350 instrument.

PS and ES were prepared by previously reported reductions of the corresponding monoorganyltrichlorosilanes with lithium aluminium hydride in di-*n*-butyl ether.[20] The identity of these compounds was confirmed by their mass spectra and their purity (better than 98%) was checked by gas chromatography. Authentic samples of silacyclobutane, methylsilane, methane, silane, ethene and ethyne were from the laboratory stock.

Results and Discussion

For the irradiation into the $\delta(H_3Si)$ mode of both $RSiH_3$ monoorganylsilanes, the most strongly absorbed lines, *i.e.* P(34) at 931.0 cm^{-1} for PS, and P(20) at 944.2 cm^{-1} for ES were chosen. Standard absorption coefficients at these wavenumbers are 0.34 kPa^{-1} cm^{-1} (PS) and 0.20 kPa^{-1} cm^{-1}(ES).

Probable steps of organylsilanes decomposition

Prop-2-enylsilane. Irradiation of PS (1.3 kPa) with a fluence of 1.0 J cm^{-2} leads to the formation of a number of gaseous products and the deposition of a grey solid. IR spectral changes of the cell content reveal formation of ethyne, methane and silane. These products and also ethene, methylsilane, propene and C_3H_4 hydrocarbons were identified by GC–MS (Fig. 1). A residual pressure in the irradiated cell after freezing these volatile compounds in a trap cooled by liquid nitrogen indicated the presence of hydrogen. The distribution of volatile products (in mol%) does not significantly change within the 20–80% decomposition progress: CH_4 (1.5–5.2), SiH_4 (3.4–10), C_2H_4 (38–48), C_2H_2 (11–18), CH_3SiH_3 (1–5.5), C_3H_6 (17–25), C_3H_4 (2–7). The use of higher fluence (a focused beam, 10 J cm^{-2}) resulted in a decrease (in mol%) of C_2H_4 (30–32) and C_3H_6 (9–10), and in an increase of C_2H_2 (34–36).

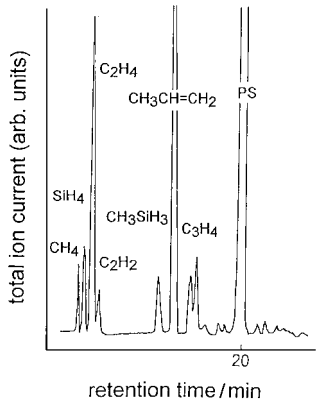

Fig. 1 Typical GC–MS trace of irradiated PS

It is known that decomposition of organosilanes $RSiH_3$ involves 1,1-H_2, 1,2-H_2, alkane and alkene elimination pathways,[21–23] and that IRMPD of alkylsilanes (R = C_2H_5, *n*-C_4H_9) proceeds *via* a four-centre activated complex including H atoms β to silicon.[24–26] It is also known that the major pathway in the complex thermal decomposition of allyltrimethylsilane[27,28] and diallyldimethylsilane[29,30] is the retroene elimination of propene. This retroene pathway cannot, however, operate with PS due to the absence of the CH_3 group. The proved occurrence of the H_2, alkane and alkene elimination channels from $RSiH_3$ would afford products of reactions (1)–(3), Scheme 1. Propyne and propadiene being undetected in our experiments implies that reaction (3) does not take place. The silylenes presumed in reactions (1) and (2) can undergo insertion into Si—H bonds or addition on double bonds to yield higher molecular products; the absence of such products indicates that these compounds undergo consecutive decomposition or polymerization/dehydrogenation.[11] The Si-containing unsaturate assumed in reaction (1) can undergo cleavage affording the C_2H_3 radical which is (i) known to prefer[31] combination into buta-1,3-diene over disproportionation into ethene and ethyne, and (ii) expected to favour [H] abstraction from H—Si bonds. The non-observation of buta-1,3-diene implies that the role of the disproportionation and combination reactions is small, and that ethene is rather produced by the abstraction of H(Si) by the C_2H_3 radical. The very large amounts of ethene make us believe that PS rearranges into silacyclobutane (SCB). This yet unreported rearrangement involves a closure at Si and 1,3-H shift and would be followed by reactions (4) and (5), Scheme 1, affording ethene and silene (major products) and propene and silylene (minor products) in accord with the reported IRMPD[32] (and also conventional decomposition[33]) of SCB. The PS rearrangement into SCB and subsequent intermediacy of silene, methylsilylene and silylene would also explain the observed formation of methylsilane and silane, steps (6) and (7), Scheme 1. The prevalence of silene and dehydrogenation of this transient (due to its likely absorption

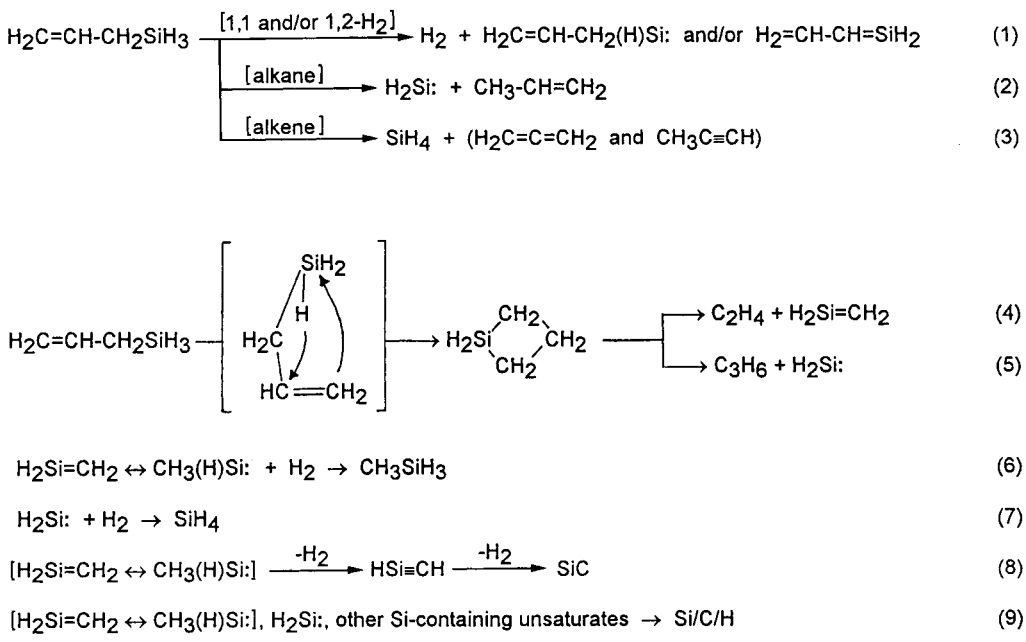

Scheme 1

Table 1 Significant[a] signals in the mass spectra of PS and SCB

	m/z															
compound	72	71	70	67	66	57	55	45	44	43	42	41	39	31	29	28
PS[b]	65	41	39	11	10	18	28	32	100	80	23	16	22	16	14	19
SCB[b]	66	39	42	10	11	19	28	32	100	79	23	15	22	14	11	22
PS[c]	96	42	47			18		18	100	35						
SCB[c]	65	28	38			10		18	100	11						

[a]Relative intensity (average of 10 data) $\geqslant 10\%$. [b]70 eV. [c]20 eV.

of the laser radiation), as well as polymerization/dehydrogenation of other transient unsaturates, reactions (8) and (9), Scheme 1, are plausible steps[32] of the IRMPD of SCB and would also explain the composition of the solid deposit produced in IRMPD of PS (see later).

In an attempt to prove the rearrangement by identifying SCB among the decomposition products, we examined the IRMPD of PS at fluences just above the IRMPD threshold (0.3 J cm^{-2}), driving the decomposition only to $<5\%$ conversion. The distribution of the products in these experiments did not, however, differ from those obtained at the high laser fluence. This finding is in accordance with commonly assumed temperature gradients inside the hot zone which facilitate low- and high-temperature steps in IR laser-induced reactions to occur concurrently. Neither experiments in which PS was irradiated in an excess of buta-1,3-diene, a known chemical trap of silenes and silylenes, helped in proving the intermediacy of $H_2Si{=}CH_2$ or $CH_3(H)Si{:}$ (and consequently of SCB), since we did not observe any butadiene adducts of these species. Nevertheless, we think that the suggested PS→SCB rearrangement is supported by the very similar mass fragmentations of both compounds at 20 and 70 eV (Table 1). It is known that fragmentation under electron impact and by heat is controlled in the same manner for many compounds; the mass spectra of both PS and SCB are not only almost identical, but they are dominated by a peak at M−24, corresponding to loss of ethene which is very charateristic for silacyclobutanes.

Ethynylsilane. IRMPD of ES has, compared to that of PS, a dramatically different course, since irradiation of ES (1.3 kPa) with a single pulse (fluence 1.3 J cm^{-2}) results in an explosive reaction accompanied with a yellow luminescence. This explosive IRMPD of ES also takes place at lower pressures when it is induced at higher fluences (Fig. 2); a non-explosive decomposition could not, in fact, be induced below the explosive threshold even with as many as several hundred pulses. ES decomposes into a mixture of ethyne (major product), ethene, methane (traces), silane (Fig. 3) and uncondensable hydrogen, along with a dark soot-like fog which deposits to form a solid film. The relative amounts of gaseous products do not change significantly under different explosive conditions (Table 2).

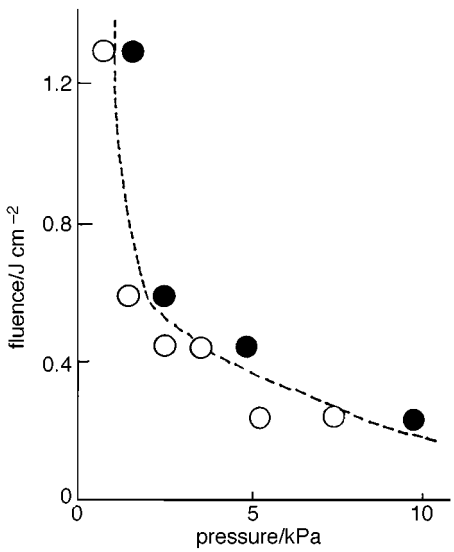

Fig. 2 Laser fluence *vs.* pressure diagram of the explosion limit for IRMPD of ES. Filled and empty circles relate to explosive reaction and no reaction, respectively.

It is known that the thermal decomposition of ES is a very complex reaction with the major dissociation route being 1,1-H_2 elimination and with some contributions from rearrangement pathways.[34,35] These plausible initial steps are given in Scheme 2. The rearrangement routes would yield $C_2H_2 + H_2Si{:}$, $H_2C{=}CH(H)Si{:}$ or $C_2H_4 + Si$ (depending upon whether the reaction is occurring *via* silirane or silirene). The observed high yield of ethyne and the very low yield of ethene together with the absence of elemental silicon in the deposit

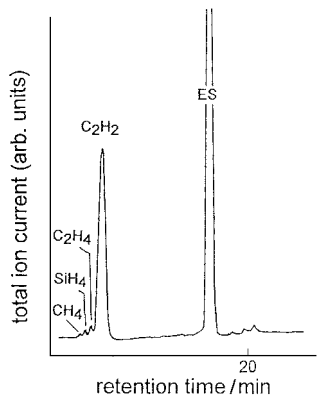

Fig. 3 Typical GC–MS trace of irradiated ES

Table 2 Typical product yield data of single-pulse IRMPD of ES

			gaseous products (mol%)		
pressure/kPa	fluence/J cm^{-2}	conversion (%)	SiH_4	C_2H_4	C_2H_2
1.30	0.25	85	8	10	82
0.70	0.45	77	5	6	89
0.30	0.60	66	4	8	88
0.16	1.30	20	7	7	86

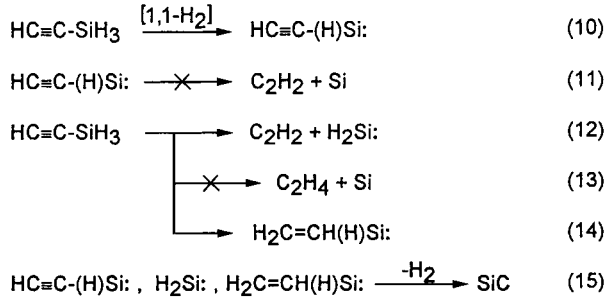

Scheme 2

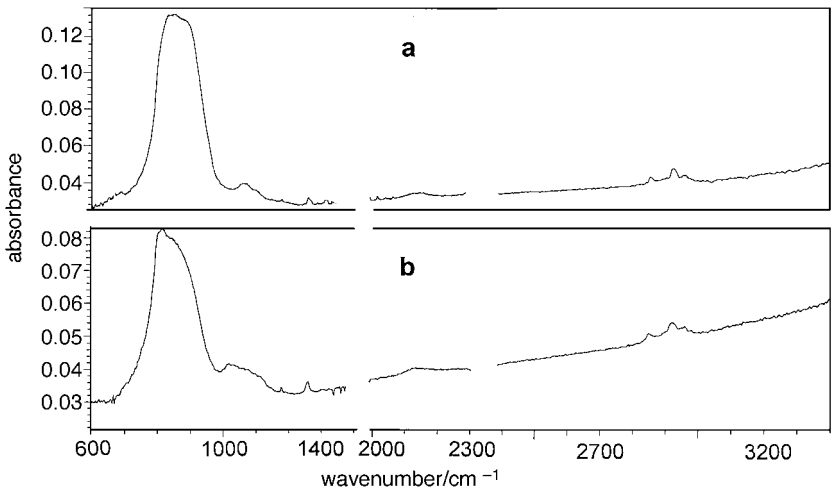

Fig. 4 Typical FTIR spectra of the deposits from ES (a) and PS (b)

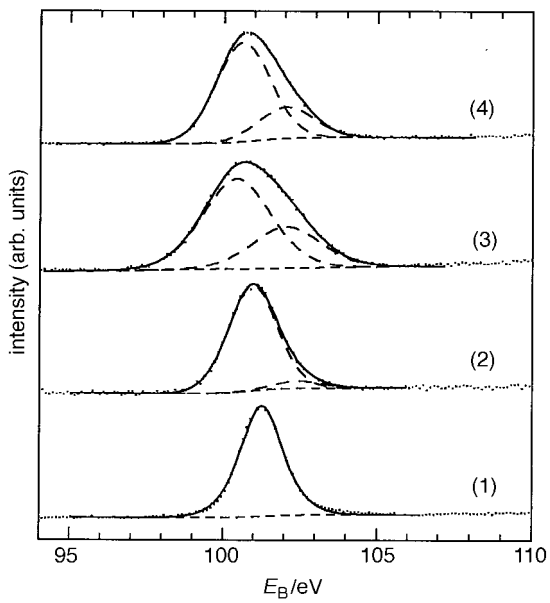

Fig. 5 Si 2p core level spectra of the deposits produced by laser irradiation of ES (1, 2) and PS (3, 4). (1, 3) Deposit as received, (2) deposit sputtered by Ar ions ($E=5$ keV, $I=30$ μA, $t=5$ min), (4) sputtered deposit ($t=2$ min).

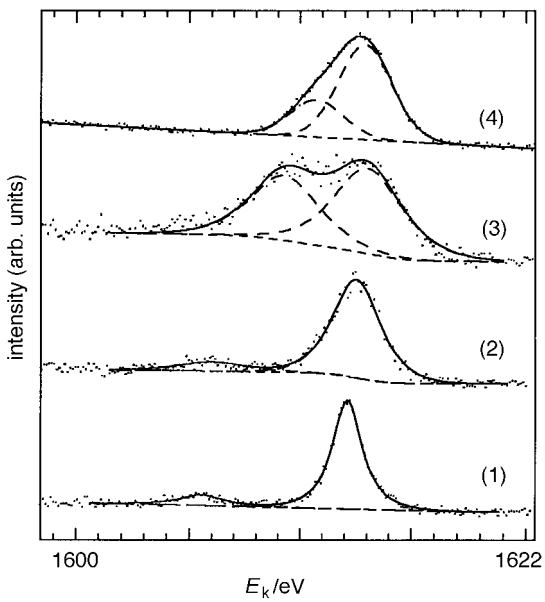

Fig. 6 Si $KL_{23}L_{23}$ Auger electron spectra of the deposits (definitions as in Fig. 5)

(see later) imply the importance of step (12), Scheme 2, and rule out steps (11) and (13). We note that ethyne predominates over ethene in the IRMPD much more than in shock tube conditions at 1100–1250 K.[34] This indicates that channel (12) is more feasible under our conditions, but any quantification of this is prevented due to the very complex nature[34] of ES decomposition. We can only assume that the main species forming the solid deposit are HC≡C-(H)Si:, H_2Si: and H_2C=CH(H)Si: unsaturates which take part in polymerization/dehydrogenation in order to produce the observed silicon carbide (see later).

Properties of the solid deposit

FTIR spectra of the deposits from both PS and ES (Fig. 4) show an almost identical pattern and consist of a dominating absorption band at 800 cm^{-1} [ν(Si—C)], a weak broad band at *ca.* 1050 cm^{-1} [probably ν(Si—O)], an almost negligible band at 2130 cm^{-1} [ν(Si—H)] and very weak bands at 2850, 2910 and 2930 cm^{-1} [ν(C—H)]. This pattern is typical for silicon carbide with low C/H and O contamination. The position of the C—H stretches is compatible with a saturated carbonaceous structure.

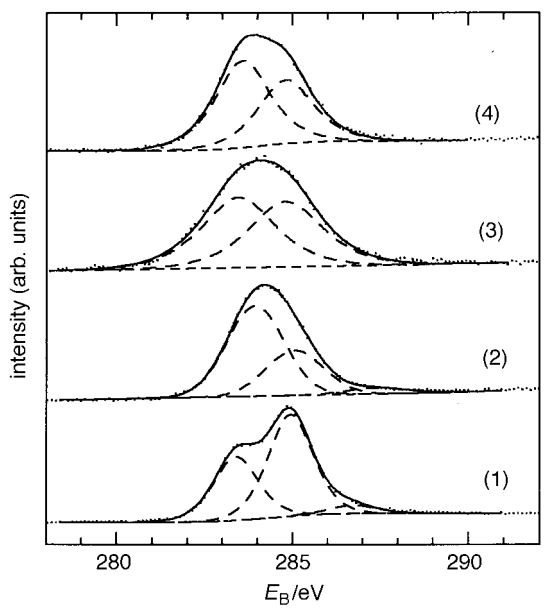

Fig. 7 C 1s core level spectra of the deposits (definitions as in Fig. 5)

The Si 2p core level spectra (Fig. 5) as well as the Si ($KL_{23}L_{23}$) Auger electron spectra (Fig. 6) of the deposits produced from ES show the presence of essentially only one chemical state of Si while two different states are observed in spectra of the deposits obtained from PS. The Si 2p core level binding energies obtained by fitting the measured spectra along with values of the modified Auger parameters calculated as a sum of the kinetic energy of Auger electrons and binding energy of Si 2p electrons are listed in Table 3. For the purpose of comparison, values measured under identical conditions for reference samples of authentic SiC and silicone resin are included. On the basis of comparison and taking into account published data[36] we can assign the observed chemical states of Si to carbidic (Si^{α}) and organosilicon (Si^{β}). In agreement with this assignment, the C 1s core level spectra (Fig. 7) reveal the presence of two chemical states of carbon, which are attributed to carbidic carbon (C^{α}) and to carbon probably belonging to an organosilicon polymer with incorporated oxygen and/or to surface contamination by adsorbed species (C^{β}). Their concentrations along with the corresponding binding energies are also listed in Table 3. The composite structure of Si 2p and Si KLL peaks of deposits arising from PS and the changes observed after ion sputtering require further discussion. It follows from comparison of the intensity ratio of the components belonging to different chemical states of Si before and after ion sputtering that the latter spectra show an increased concentration of silicon carbide. This difference suggests sample inhomogeneity in the direction normal to the surface. This inhomogeneity is partly due to the interaction of the sample surface with the ambient atmosphere during trans-

Table 3 The Si 2p, C 1s and O 1s core level binding energies (E_B) of the fitted photoemission lines, modified Auger parameters (α') and calculated atomic concentrations (c) of individual chemical states of elements

	E_B/eV					α'		c				
precursor	Si 2p		C 1s		O 1s	Si^{α}	Si^{β}	Si^{α}	Si^{β}	C^{α}	C^{β}	O
ES	101.2		283.4	284.8	532.5	1714.7		1.00		0.81	1.29	0.19
ES[a]	101.0		283.7	284.4	532.4	1715.0		1.00		1.05	0.52	0.17
PS	100.5	102.1	283.5	284.4	532.2	1715.1	1712.9	0.70	0.30	0.78	0.73	0.78
PS[b]	100.6	102.0	283.6	284.4	532.1	1715.1	1710.5	0.76	0.24	0.71	0.68	0.37
SiC[c]	100.1	103.0	282.2	284.4	532.4	1714.2	1710.5	0.81	0.19	0.70	0.62	0.57
silicone resin		102.4		285.8	532.4		1711.3		1.00		2.00	1.00

[a]Sample sputtered by argon ions ($E = 5$ keV, $I = 30$ μA, $t = 5$ min). [b]Sample sputtered by Ar ions for 2 min. [c]Authentic sample of silicon carbide, 400 mesh (Aldrich).

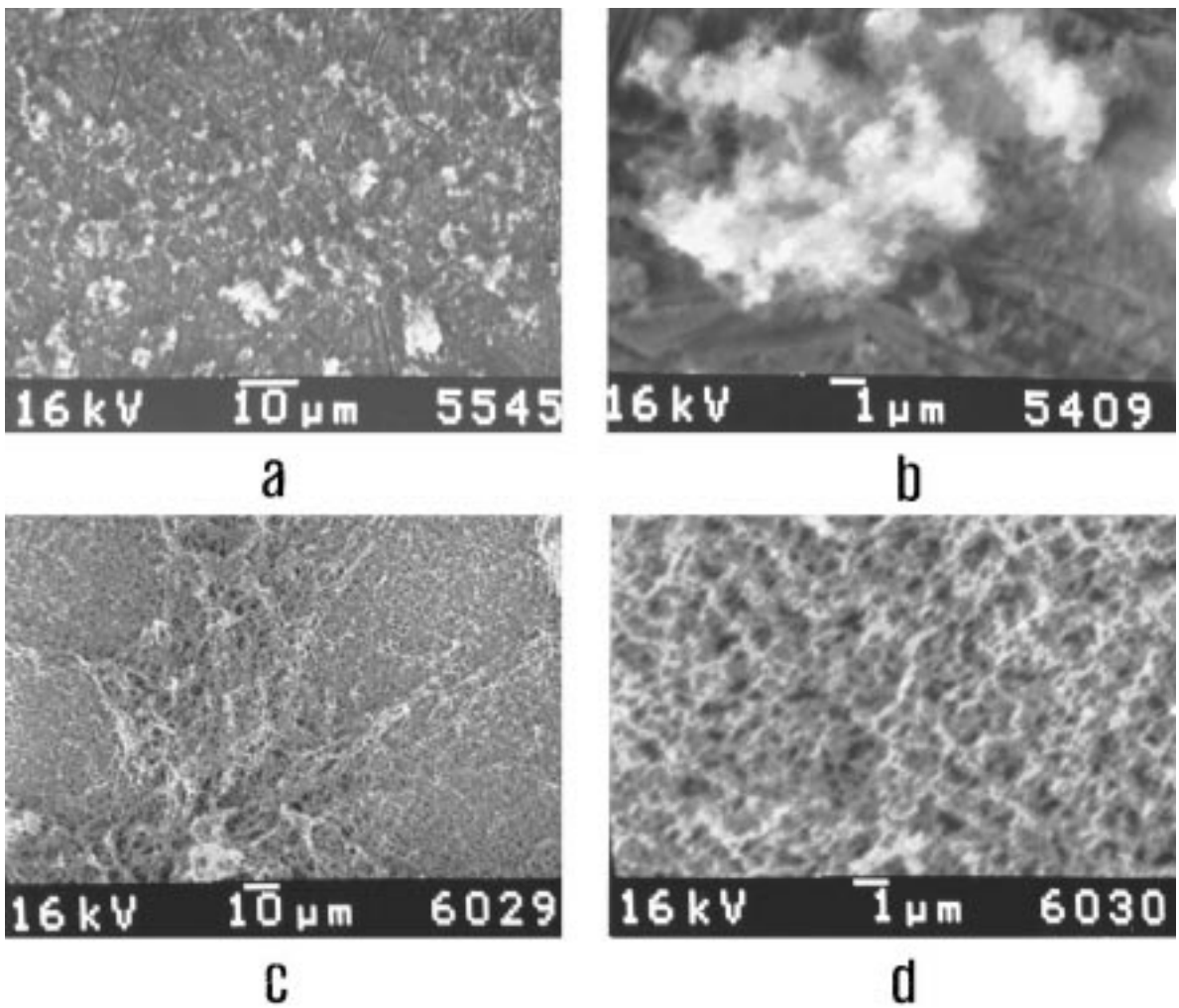

Fig. 8 Typical SE micrographs of the deposits produced from PS (a, b) and ES (c, d)

port from the reactor to the electron spectrometer. The changes in C 1s spectra (Fig. 7) induced by argon ion sputtering are consistent with the removal of species adsorbed on the deposit surface from the gas reaction mixture, the presence of which is a likely source of additional inhomogeneity.

The Si 2p and C 1s core electron binding energies measured for deposits are slightly higher than the values observed for the reference sample of SiC (Table 3). Qualitatively, the same shift is observed for the modified Auger parameter, showing thus that it can not be due to an improper choice of reference level or charging effects. Besides, the deposit produced from ES was electrically conducting and consequently did not charge during spectral measurement. The observed shifts are characteristic of amorphous and highly dispersed materials.[37] In agreement with this view is the finding[38] that the C 1s binding energy increases from 282.5 to 283.4 eV after ion sputtering of α-SiC. The latter value is similar to that measured for our deposits which, in turn, does not change on sputtering. It is well known that ion sputtering produces a significant concentration of surface defects leading ultimately to a quasi-amorphous structure.[39]

SEM analyses of the deposits from ES and PS (Fig. 8) reveal their different morphology. The films from ES which are essentially SiC show a woven texture, while those from PS consisting of SiC and Si/C/H involve agglomerates of size *ca.* 1–10 μm. The bulkier particles from PS confirm the importance of the gas-phase polymerization; the continuous nets observed with ES seem to indicate that SiC particles agglomerate after having been deposited. Adhesion of the deposited films to the substrates kept at room temperature is rather low, but can be increased by annealing.

The presence of the oxygen in the deposit from PS in relatively higher amounts compared to that from ES may be explained by incorporation of oxygen in the Si/C/H polymer. Considering the well known inertness of SiC, we assume that the polymer formed from very reactive Si-containing unsaturates (see above) exhibits residual reactivity due to a small content of Si=C bonds.[40] On the other hand, the presence of comparable amounts of oxygen in superficial layers of an SiC reference sample indicates that partial surface oxidation of carbide during its exposure to ambient atmosphere can take place.

Conclusion

We conclude that IRMPD of prop-2-enylsilane and ethynylsilane is a convenient process for deposition of Si/C phases. We pointed out earlier[13] that small differences in the structure of the $RSiH_3$ precursor can lead to different structures of the deposited material. This convenient way of modifying the structures of the deposited layers and optimizing the process for production of SiC (or Si/C/H phases with high SiC content) using structurally different precursors is demonstrated in this work: the IRMPD of prop-2-enylsilane is a multi-pulse process yielding Si/C/H phases with a high content of SiC, while IRMPD of ethenylsilane is an explosive single-pulse process affording exclusively SiC. The latter process uses a readily handled precursor and is promising for the deposition of SiC films at substrates kept at relatively low temperatures.

This work was supported by the grant of the Academy of Sciences of the Czech Republic (grant no. A4072509). The authors thank Ing. I. Spirovova for assistance in XPS measurements.

References

1 J. A. O'Neil, M. Horsburg, J. Tann, K. J. Grant and G. L. Paul, *J. Am. Ceram. Soc*., 1989, **72**, 1130.
2 A. E. Kaloyeras, J. W. Corbett, P. J. Toscano and R. B. Rizk, *Mater. Res. Soc. Symp. Proc*., 1990, **192**, 601.
3 H. Schmidbaur, R. Hager and J. Zech, in *Frontiers of Organosilicon Chemistry*, ed. A. R. Bassindale and P. P. Gaspar, The Royal Society of Chemistry, Cambridge, 1991, p. 62.
4 E. F. Hennge, in *Abstracts of Lectures, Xth International Symposium on Organosilicon Chemistry*, Poznan, Poland, 1993, p. 42.
5 J. M. Agullo, F. Fau-Canillac and F. Maury, *J. Mater. Chem*., 1994, **4**, 695.
6 J. Pola, H. Beckers and H. Bürger, *Chem. Phys. Lett*., 1991, **178**, 192.
7 J. Pola, Z. Bastl, J. Tláskal, H. Beckers, H. Bürger and P. Moritz, *Organometallics*, 1993, **12**, 172.
8 V. Dřínek, Z. Bastl, J. Šubrt, M. Urbanová and J. Pola, *Proc SPIE-Int. Soc. Opt. Eng*., 1994, **2461**, 121.
9 J. Pola, J. P. Parsons and R. Taylor, *J. Organomet. Chem*., 1993, **489**, C9.
10 M. Urbanová, E. A. Volnina, L. E. Gusel'nikov, Z. Bastl and J. Pola, *J. Organomet. Chem*., 1996, **509**, 73.
11 Z. Bastl, H. Bürger, R. Fajgar, D. Pokorná, J. Pola, M. Senzlober, J. Šubrt and M. Urbanová, *Appl. Organomet. Chem*., 1996, **10**, 83.
12 V. M. Scholz, W. Fuss and K-L. Kompa, *Adv. Mater*., 1993, **5**, 38.
13 J. Pola, Z. Bastl, J. Šubrt, J. R. Abeysinghe and R. Taylor, *J. Mater. Chem*., 1996, **6**, 155.
14 M. Santos, L. Díaz, Z. Bastl, V. Hulínský, M. Urbanová, J. Vítek and J. Pola, *J. Mater. Chem*., 1996, **6**, 975.
15 D. A. Shirley, *Phys. Rev*., 1972, **85**, 4709.
16 A. E. Hughes and B. A. Sexton, *J. Electron Spectrosc. Relat. Phenom*., 1988, **46**, 31.
17 J. H. Scofield, *J. Electron Spectrosc. Relat. Phenom*., 1976, **8**, 129.
18 M. P. Seah in *Practical Surface Analysis. Vol. 1. Auger and X-Ray Photoelectron Spectroscopy*, ed. D. Briggs and M. P. Seah, J. Wiley & Sons, Chichester, 1990, p. 201.
19 M. P. Seah and W. A. Dench, *Surf. Interface Anal*., 1979, **1**, 1.
20 V. Bažant, V Chvalovský and J. Rathouský, *Organosilicon Compounds*, Academia, Prague, 1965.
21 P. S. Neudorfl, E. M. Lown, I Safarik, A. Jodhan and O. P. Strausz, *J. Am. Chem. Soc*., 1987, **109**, 5780.
22 B. A. Sawrey, H. E. O'Neal, M. A. Ring and D. Coffey, *Int. J. Chem. Kinet*., 1984, **16**, 7; 801.
23 S. F. Rickborn, M. A. Ring, H. E. O'Neal and D. Coffey, *Int. J. Chem. Kinet*., 1984, **16**, 289.
24 J. S. Francisco, S. A. Joyce, J. I. Steinfeld and F. Walsh, *J. Phys. Chem*., 1984, **88**, 3098.
25 D. M. Rayner, R. P. Steer, P. A. Hackett, C. L. Wilson and P. John, *Chem. Phys. Lett*., 1986, **123**, 449.
26 J. W. Thoman and J. I. Steinfeld, *Chem. Phys. Lett*., 1986, **124**, 35.
27 W. J. Bailey and M. S. Kaufmann, *Chem. Eng. News*, 1969, **47**, 35.
28 T. J. Barton, S. A. Burns, I. M. T. Davidson, S. Ijadi-Maghsoodi and I. T. Wood, *J. Am. Chem. Soc*., 1984, **106**, 6367.
29 E. Block and L. K. Revelle, *J. Am. Chem. Soc*., 1978, **100**, 1630.
30 N. Auner, I. M. T. Davidson and S. Ijadi-Maghsoodi, *Organometallics*, 1985, **4**, 2210.
31 M. J. Gibian and R. C. Corley, *Chem. Rev*., 1973, **73**, 441.
32 Z. Bastl, H. Bürger, R. Fajgar, D. Pokorná, J. Pola, M. Senzlober, J. Šubrt and M. Urbanová, *Appl. Organomet. Chem*., 1996, **10**, 83.
33 I. M. T. Davidson, A. Fenton, S. Ijadi-Maghsoodi, R. J. Scampton, N. Auner, J. Grobe, N. Tillman and T. J. Barton, *Organometallics*, 1984, **3**, 1593 and references therein.
34 D. S. Rogers, M. A. Ring and H. E. O'Neal, *Organometallics*, 1986, **5**, 1521.
35 J. J. W. McDouall, H. B. Schlegel and J. S. Francisco, *J. Am. Chem. Soc*., 1989, **111**, 4622.
36 *NIST X-ray Photoelectron Spectroscopy Database*, NIST Std. Ref. Database 20, US Dept. of Commerce, Gaithersburg, 1989.
37 W. G. Egelhoff Jr., *Surf. Sci. Rep*., 1987, **6**, 253.
38 K. L. Smith and K. M. Black, *J. Vac. Sci. Technol. A*, 1984, **2**, 744.
39 R. Kelly, in *Ion Bombardment Modification of Surfaces*, ed. O. Auicello and R. Kelly, Elsevier, Amsterdam, 1984, p. 79.
40 I. M. T. Davidson, C. E. Dean and F. T. Lawrence, *J. Chem. Soc., Chem. Commun*., 1981, 52.

Paper 7/00370F; *Received* 15*th January*, 1997